

3-Aminopyrrolidine lithium amides as chiral ligands for alkyllithium derivatives: Synthesis, NMR analysis, and computational study of their mixed aggregates*

Anne Harrison-Marchand¹, Jean-Yves Valnot¹, Aline Corruble¹,
Nicolas Duguet¹, Hassan Oulyadi², Stéphanie Desjardins²,
Catherine Fressigné^{1,3}, and Jacques Maddaluno^{1,‡}

¹Laboratoire des Fonctions Azotées et Oxygénées Complexes, IRCOF,
UMR 6014 CNRS, Université de Rouen, 76821 Mont Saint-Aignan Cédex, France;

²Laboratoire de Chimie Organique et Biologique Structurale, IRCOF,
UMR 6014 CNRS, Université de Rouen, 76821 Mont Saint-Aignan Cédex, France;

³Laboratoire de Chimie Théorique, UMR 7616 CNRS, Université Pierre and Marie
Curie, 4 place Jussieu, 75252 Paris Cédex 05, France

Abstract: An overview of the role of 3-aminopyrrolidine lithium amides (3-APLi's) as chiral ligands for alkyllithiums (AlkLi's) is presented. Synthetic developments as well as NMR characterizations and computational interpretations have been simultaneously and complementarily conducted to improve the ligand design for a model reaction that is the condensation of AlkLi's on *o*-tolualdehyde, for which enantiomeric excesses up to 80 % were obtained. This study describes the whole chain going from the synthesis of the chiral 3-aminopyrrolidines (3-APs) (18 different 3-APs synthesized) to the characterization of the noncovalent mixed aggregates resulting from the interaction between the organolithium partners (3-APLi:AlkLi). Finally, the docking of the aldehyde on one lithium of the aggregate was analyzed by theoretical means on simplified models, in an attempt to understand the structure of the fully loaded pretransition complexes.

Keywords: organolithium; enantioselectivity; chiral lithium amide; pyrrolidine; nucleophilic addition; DFT calculations; multinuclear NMR.

INTRODUCTION

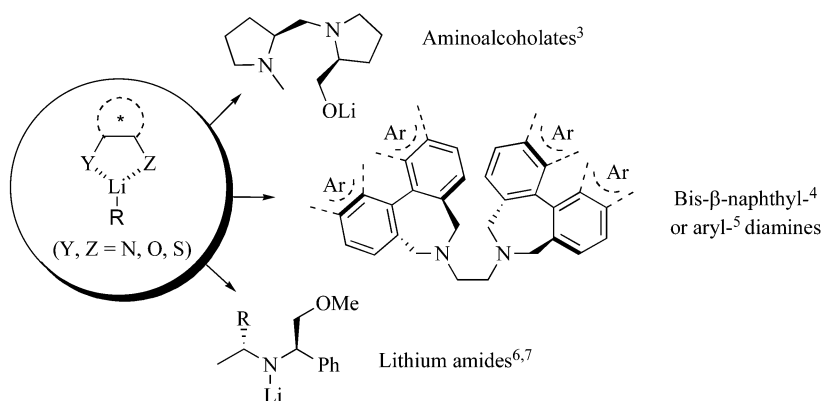
Fine-tuning the balance between reactivity and selectivity is certainly one of the current challenges faced by asymmetric synthesis, now at work in the arena of chemical catalysis. Controlling the trajectory of a reagent while preserving its chemical activity is often a matter of fitting a square peg in a round hole. Dimmed reagents becoming simultaneously chiral and active are expected to offer a solution to this problem. Organometallic species are particularly apt to these manipulations because of such specific physicochemical parameters as the aggregation and solvation levels. Thus, a chiral coordinating entity suitable to transform an oligomer into a smaller analog [1] is to be regarded as a potential cat-

*Pure Appl. Chem. **78**, 197–523. An issue of reviews and research papers based on lectures presented at the 13th IUPAC International Symposium on Organometallic Chemistry Directed Towards Organic Synthesis (OMCOS-13), Geneva, Switzerland, 17–21 July 2005.

‡Corresponding author

alytic partner. Organozinc reagents afford a remarkable illustration of this concept, and hundreds of chiral ligands, in particular amino alcohols [2], have been found to transform these sluggish nucleophiles into “magic bullets” able to differentiate between the enantiofaces of aldehydes, even when employed in substoichiometric amounts.

In this context, routine organometallic species such as organolithium or Grignard reagents hardly find their place. The balance is this time displaced on the reactivity side, and funneling these highly nucleophilic entities through an enantio-differentiating process is difficult. Actually, little is known about the enantioselective addition of organolithiums on “classical” electrophiles such as ketones or aldehydes, even if this condensation is probably one of the more usual ways of making a C–C bond. Three classes of chiral reagents have been found to influence the stereochemical outcome of this reaction (Scheme 1), these are the lithium amino alcoholates [3], tertiary diamines [4,5], and lithium amides [6,7].

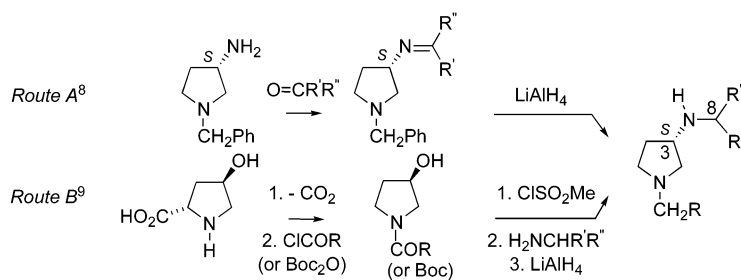


Scheme 1

All structures cited above probably share a common chelating pattern, with the lithium cation belonging to a five-membered metallacycle. Another common point is the “tight” experimental conditions in which high enantiomeric excesses (ee’s) could be obtained (below $-100\text{ }^{\circ}\text{C}$ and in specific solvent mixtures such as DMM:Et₂O 1:1). This latter observation may constitute a drawback to the applications of these systems. Thus, the development of new chiral ligands that are easily accessible and able to afford acceptably high induction levels in more “classical” conditions, that is to say, in one single solvent (THF, Et₂O, or toluene) and not below $-78\text{ }^{\circ}\text{C}$, remains a challenge.

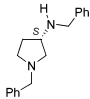
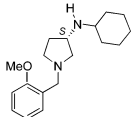
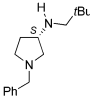
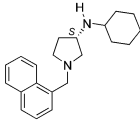
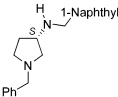
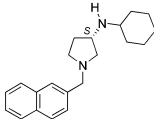
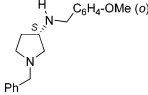
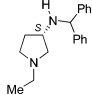
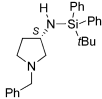
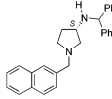
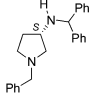
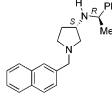
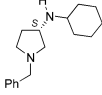
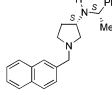
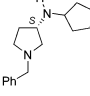
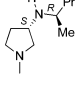
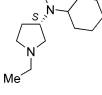
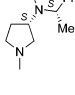
SYNTHESES OF CHIRAL 3-AMINOPYRROLIDINES

We have been interested for a while in the use of chiral lithium amides derived from 3-aminopyrrolidines (3-APs) as chiral ligands for organolithium reagents. Two main syntheses have been developed (Scheme 2, routes A [8] and B [9]) which led to 18 different 3-APs. The structures and overall yields are gathered in Table 1. Note that the 3-APs bear either one (at C³, **1–14**) or two (at C³ and C⁸, **15–16**) stereogenic center(s) and their ee is >95 % in all cases.



Scheme 2

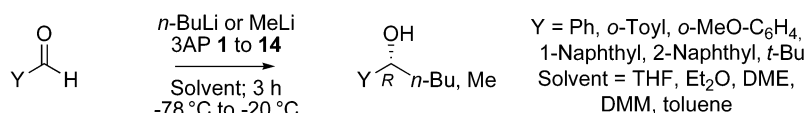
Table 1 3-APs obtained through the two synthetic routes of Scheme 2.

3AP	Route		Yd %	3AP	Route		Yd %
	1	A	91		10	B	38
	2	A	94		11	B	40
	3	A	91		12	B	50
	4	A	84		13	B	30
	5	A	56*		14	B	24
	6	A	69		15a	B	15-20
	7	A	75		15b	B	15-20
	8	A	53		16a	B	35
	9	B	32		16b	B	33

*Prepared from 3-amino-N-benzylpyrrolidine and Ph₂t-BuSiCl.

APPLICATIONS OF 3-AMINOPYRROLIDINE LITHIUM AMIDES AS CHIRAL LIGANDS FOR ALKYL LITHIUM IN THE ENANTIOSELECTIVE NUCLEOPHILIC ALKYLATION OF ALDEHYDES

We decided to focus on the hydroxyalkylation of nonenolizable aldehydes as a model enantioselective reaction. Starting from a standard procedure described in the literature [10], we showed that the ratio lithium amide:organolithium:aldehyde = 1.5:2.5:1.0 was the most effective to attain both optimal yields and ee's. Six different aldehydes (benzaldehyde, *o*-tolualdehyde, *o*-anisaldehyde, 1-naphthaldehyde, 2-naphthaldehyde, and pivalaldehyde) were reacted with *n*-butyllithium or methylolithium for 3 h, the solvent being THF, Et₂O, DME, DMM, or toluene while the temperature was varied from -78 to -20 °C [9a]. The diamines **1** to **14** (one single *S* stereogenic center on C³) were initially compared to optimize the reaction conditions (Scheme 3).



Scheme 3

Preliminary investigations implied that *o*-tolualdehyde and THF were the best substrate and solvent, respectively, to reach significant inductions. The results obtained with the 14 diamines considered suggested that the influence of the substituent on the intracyclic nitrogen was relatively meaningless. Only 3-APLi's bearing a hindered lateral amino-chain led to acceptable chemical yields and ee's. Thus, amines **6** to **14** provided the butylated alcohol in ee's higher than 50 %, at -78 °C (Table 2). Comparable results were obtained for MeLi and *n*-BuLi. The *R* alcohols were recovered in all cases.

Table 2 Enantioselective hydroxyalkylation of *o*-tolualdehyde by *n*-BuLi in the presence of **6Li–14Li**.

3-APLi	<i>t</i> (h)	Conv. (%)	ee (%)
6Li	4	77	73
7Li	3	72	67
8Li	3	63	63
9Li	3	72	63
10Li	3	71	60
11Li	3	65	50
12Li	3	67	74
13Li	3	66	64
14Li	3	98	64

The temperature has a dramatic effect on the outcome of this reaction. We have established, on both chemical and, recently, spectroscopic grounds, that the aggregation between the lithium amide and the nucleophile has to be performed at -20 °C for at least 30 min. The resulting reaction mixtures have then to be cooled at -78 °C before addition of the aldehyde.

The influence of a second stereogenic center (C⁸) introduced on the lateral amino chain was studied at this point. Thus, 3-AP **15** and **16** were employed in the nucleophilic addition of *n*-BuLi on *o*-tolualdehyde, in THF, at -78 °C for 1 to 2 h, according to the above procedure. The results are gathered in Table 3.

Table 3 Enantioselective hydroxyalkylation of *o*-tolualdehyde by *n*-BuLi in the presence of 3-APLi **15Li** and **16Li**.

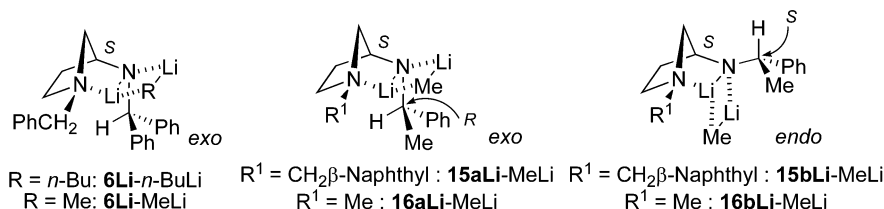
3-APLi	t (h)	Conv. (%)	ee (%)	Alcohol
15aLi	1	95	77	<i>R</i>
15bLi	1	91	51	<i>S</i>
16aLi	2	97	80	<i>R</i>
16bLi	2	98	74	<i>S</i>

Diamines **15a,b** and **16a,b** led to ee's up to 80 %. Interestingly, the sense of the induction appeared to depend on the configuration of the second stereogenic center. Indeed, while the (3*S*,8*R*)-3-APs **15a** and **16a** was in favor of alcohol *R*, the *S* enantiomer was mainly formed in the presence of the (3*S*,8*S*)-3-APs **15b** and **16b**. This observation suggested that, in this case, the sense of induction was driven by the second stereogenic center, dimming that of the original C³. The racemic analogs at C³ of **16a** (i.e., 3*S*,8*R*/3*R*,8*R*) and **16b** (i.e., 3*S*,8*S*/3*R*,8*S*) were then synthesized [11] to further clarify this phenomenon. Accordingly, the hydroxyalkylations of *o*-tolualdehyde with *n*-BuLi led to similar ee's and inductions with **16a,b** or their racemic analogs.

SPECTROSCOPIC CHARACTERIZATION OF THE MIXED AGGREGATES

A systematic NMR characterization of the mixed aggregates was undertaken to identify the intermediates into solution, in an attempt to fine-tune the 3-AP structures. The systematic ⁶Li (*I* = 1) and occasional ¹⁵N (*I* = 1/2) labeling of these entities afforded a set of mono- and bidimensional experiments relying either on homo- or hetero- (¹H-⁶Li, ⁶Li-¹⁵N, and ⁶Li-¹³C) [9b,12] nuclear couplings [13]. The spectra of the 3-AP lithium amides alone are not displayed here since these entities tend to form unidentified oligomers in THF, associated to entangled ¹H and ⁶Li signals [9b]. However, in two cases, these amides were shown to adopt a folded pattern similar to that described below. Note also that lithium amides with "little" R' and R" tend to add in 1,2 on the carbonyl, providing α-amino alcoholates that decompose back into the starting aldehyde and amine upon work-up [8b].

We established that the 3-APLi-alkyllithium mixed aggregates form robust 1:1 noncovalent complexes organized around a quadrilateral C–Li–N–Li core (Fig. 1) in coordinating solvents such as THF or Et₂O [12,14]. The ¹³C signal of the *ipso*-carbon of the AlkLi, which appears as a 1:2:3:2:1 quintet due to the coupling with the two ⁶Li nuclei, and the ⁶Li–⁶Li couplings observed in several cases are other evidence of the formation of these complexes [9b,12]. Note that similar aggregates involving another chiral lithium amide and *n*-butyllithium have been described before by Hilmersson and Davidsson [7].

**Fig. 1**

To understand the origin of the selectivity reversal imposed by the lateral chain of the 3-APs bearing two asymmetric centers, we undertook a similar study on **15Li-MeLi** and **16Li-MeLi**. The results are shown below for **16a** (Fig. 2a) and **16b** (Fig. 2b) [9b]. Interestingly, comparable 1:1 aggregates form

with MeLi and (3*S*,8*R*) **16a** or (3*S*,8*S*) **16b**. However, the arrangements of these complexes are quite different: while **16a** provides an *exo* arrangement (Fig. 1, middle) similar to that characterized for **6Li**-*n*-BuLi and **6Li**-MeLi (Fig. 1, left), the aggregate of **16b** adopts an *endo* topology (Fig. 1, right). Note that these two arrangements correspond to the *S* and *R*, respectively, absolute configuration for the “quaternarized” lateral nitrogen.

The puckering of the pyrrolidine ring of **16a** is evidenced on the heteronuclear Overhauser effect spectroscopy (HOESY) [15] spectrum (Fig. 2a) by the Li¹-Me⁶ correlation, while the Li²-H² cross-peak characterizes the *exo* noncovalent arrangement. On the other hand, the Li²-H⁴ and Li²-H⁵ correlations observed on the HOESY spectrum of **16b** (Fig. 2b) indicate an *endo* arrangement for the aggregate. Both the ¹H-¹H NOESY spectra [9b] (not shown) and observation of a coupling constant [¹J(⁶Li, ¹⁵N) = 2.5 Hz] in the monodimensional ⁶Li spectrum for intracyclic ¹⁵N-labeled **15b** corroborate these structure assignments [16].

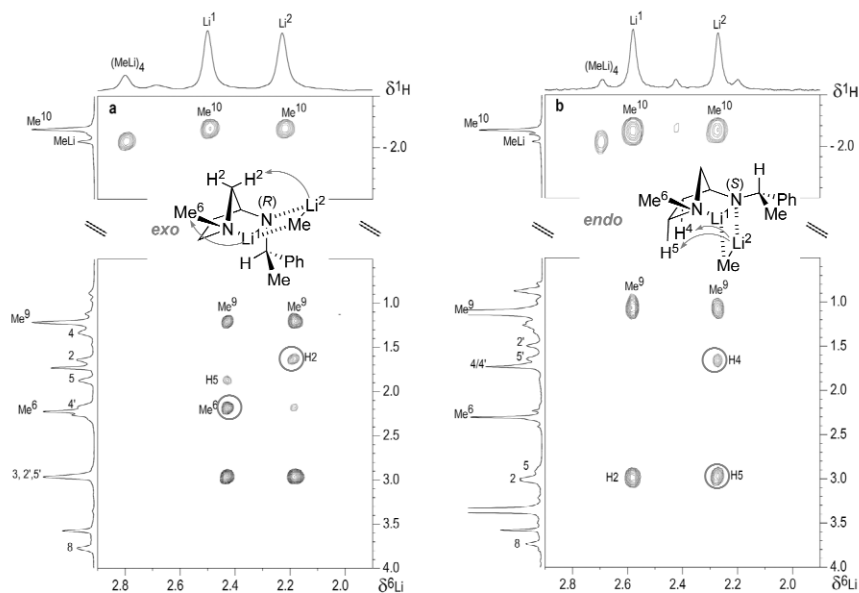
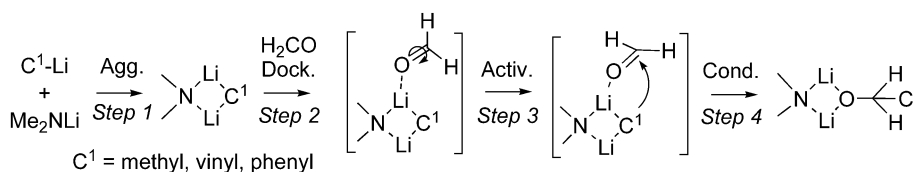


Fig. 2 HOESY spectrum of **16a**-MeLi (a, left) and **16b**-MeLi (b, right).

THEORETICAL CONSIDERATIONS

A crucial piece of information, not available from spectroscopy yet, is the approach and docking of the aldehyde on the above mixed aggregates. It has been established, in the case of the condensation of *n*-butyllithium with benzaldehyde in THF that, even at low temperatures, the reaction is too fast for NMR data to be acquired before completion [17]. In particular, the complex expected to form between an organolithium and an aldehyde preliminary to the C-C bond formation has never been characterized to our knowledge. To date, quantum mechanics seems the only way to get an insight in the interactions between the partners all along the reaction pathway. Density functional theory (DFT) methods have been shown to be appropriate and time-saving tools for the study of such organometallic entities [18]. We have focused our own work on the docking of formaldehyde on simple models (in vacuum and at 0 K) of mixed dimers involving sp³ or sp² organolithium reagents and lithium dimethylamide [19]. The typical reaction we have studied is represented in Scheme 4. In the chiral version of the reaction, the sense of the induction is determined by the sense of the rotation of the aldehyde around its C=O bond.



Scheme 4

Let us now consider the approach of the partners. Two long-distance interactions are of prime importance: the oxygen–lithium coordination and the tendency for the nucleophile to follow a Bürgi–Dunitz-type trajectory with respect to the carbonyl target. Tables 4 and 5 present a set of geometrical parameters employed to describe the intermediate complexes and the transition states for the six mixed-aggregate models considered. In all cases, the coordination of the aldehyde on the aggregate leads to a complex. The figures in Table 4 indicate that the aldehyde interacts with the lithium cation through one of the lone pairs of the oxygen. The coordination takes place within the plane of the aldehyde ($\text{H}^3\text{C}^3\text{OLi} \approx 0$) and at $\approx 120^\circ$ of the $\text{C}=\text{O}$ bond (see C^3OLiC^1 values). The data in the C^3OLiC^1 column suggest that the carbon C^1 tends also to lie in plane π (Scheme 5). Note that the aldehyde CH_2 appendage can also be oriented toward the amide nitrogen. In this case, the resulting product will be a lithium α -amino alcoholate instead of the expected lithium alcoholate (*vide supra*) [20]. The *N*-side complexes present geometrical characteristics close to the *C*-side ones.

Table 4 Geometrical parameters in post-docking complexes on mixed aggregates of lithium dimethylamide. Atom numbering in Scheme 5.

Complex	C^3OLi	$\text{H}^3\text{C}^3\text{OLi}$	C^3OLiC^1	C^3OLiN
$\text{CH}_3\text{Li}/\text{LiNMe}_2^{\text{a}}$	122	0	1	–
$\text{CH}_2=\text{CHLi}/\text{LiNMe}_2^{\text{a}}$	118	1	17	–
$\text{C}_6\text{H}_5\text{Li}/\text{LiNMe}_2^{\text{a}}$	122	0	1	–
$\text{CH}_3\text{Li}/\text{LiNMe}_2^{\text{b}}$	112	0	–	0
$\text{CH}_2=\text{CHLi}/\text{LiNMe}_2^{\text{b}}$	112	0	–	4
$\text{C}_6\text{H}_5\text{Li}/\text{LiNMe}_2^{\text{b}}$	113	0	–	2

^a*C*-side complex (see text).

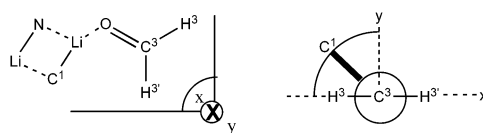
^b*N*-side complex (see text).

Table 5 Geometrical parameters in transition states involving mixed aggregates of lithium dimethylamide. Atom numbering in Scheme 5.

Entry	Transition states	$\text{C}^1\text{C}^3\text{OH}^3$	$\text{H}^3\text{C}^3\text{OLi}$	$\text{C}^1\text{C}^3\text{O}$
1	$\text{CH}_3\text{Li}/\text{LiNMe}_2^{\text{a}}$	74	59	93
2	$\text{CH}_2=\text{CHLi}/\text{LiNMe}_2^{\text{a}}$	70	59	94
3	$\text{C}_6\text{H}_5\text{Li}/\text{LiNMe}_2^{\text{a}}$	83	81	100
4	$\text{CH}_3\text{Li}/\text{LiNMe}_2^{\text{b}}$	38 ^c	22	70 ^c
5	$\text{CH}_2=\text{CHLi}/\text{LiNMe}_2^{\text{b}}$	55 ^c	51	93 ^c
6	$\text{C}_6\text{H}_5\text{Li}/\text{LiNMe}_2^{\text{b}}$	56 ^c	52	92 ^c

^{a,b}As in Table 4.

^cThe amide nitrogen is considered instead of C^1 .



Scheme 5

At the transition-state level (Table 5), the $C^1C^3OH^3$ values imply that in all cases, except entry 4, the TS corresponds to a large rotation of the aldehyde out of its original plane, a result making full sense for these early reactions. The “unusually” low $C^1C^3OH^3$ angle calculated for the MeLi–Me₂NLi aggregate is difficult to explain. Except in entry 3, the H^3C^3OLi and C^1C^3O columns indicate that C¹ attacks along a trajectory which is quite different from the ideal Bürgi–Dunitz 90/109° values. One should keep in mind that these rules apply to neutral nucleophiles, but are necessarily violated by the organometallic reagents in which an oxygen–metal interaction takes place simultaneously to the C–C bond formation [21].

Energywise, the six aggregates behave relatively similarly (Table 6 and Scheme 6). Their aggregation (Scheme 4, step 1) is exothermic by more than 50 kcal mol^{–1}, and the docking of formaldehyde (step 2) is characterized by a 14–18 kcal mol^{–1} further stabilization. From there, a low-lying transition state (step 3) is reached in less than 5 kcal mol^{–1}, low values associated to the simple rotation of the aldehyde around its C=O bond (see above). Note that the activation barriers (E^\ddagger) are always larger for the C–C than the C–N bond formation. The condensation (step 4) ends up the reaction in a large exothermic way (37–42 kcal mol^{–1} for the C–N creation vs. 57 kcal mol^{–1} for the C–C creation).

Table 6 Energies associated to the four steps of the reaction in Scheme 4 (kcal mol^{–1}).

Dimer ^a	$E(\text{agg.})^b$	$E(\text{dock})^c$	E^\ddagger^d	$E(\text{cond.})^e$
CH ₃ Li/LiNMe ₂	–52.4	–15.3	+4.6	–57.5
CH ₂ =CHLi/LiNMe ₂	–56.3	–14.9	+3.2	–57.8
C ₆ H ₅ Li/LiNMe ₂	–54.7	–17.6	+4.3	–57.7
CH ₃ Li/LiNMe ₂	–52.4	–16.8	+1.9	–37.3
CH ₂ =CHLi/LiNMe ₂	–56.3	–14.8	+2.5	–41.8
C ₆ H ₅ Li/LiNMe ₂	–54.7	–15.1	+2.6	–41.9

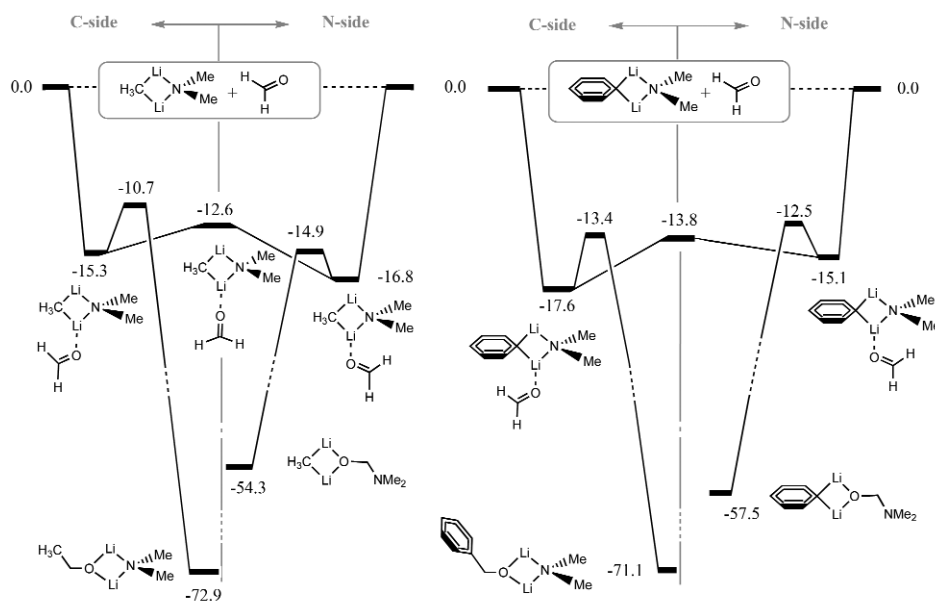
^aC-side or N-side complex (see text and Table 4).

^b $E(\text{agg.}) = E(\text{opt. aggregate}) - E(C^1Li) - E(Me_2NLi)$.

^c $E(\text{dock}) = E(\text{post-docking complex}) - E(\text{aggregate}) - E(HCHO)$.

^d $E^\ddagger = E(\text{TS}) - E(\text{post-docking complex})$.

^e $E(\text{cond.}) = E(\text{prod.}) - E(\text{TS})$.



Scheme 6 Energy diagrams for the two possible routes of the reaction between the heterogeneous dimers of methyllithium (left) or phenyllithium (right) and lithium dimethylamide with formaldehyde.

CONCLUSION

The results gathered in this paper suggest that the lithium amides derived from 3-APs can act as good chiral inductors in the condensation of AlkLi compounds on nonenolizable aldehydes. These ligands provide ee's up to 80 % in this model reaction and are easily prepared following a two- to five-step procedure. Interestingly, the sense of the induction becomes entirely controlled by the presence of an asymmetric center on the lateral chain borne by the 3-amino group. This occurs via the strict control of the topology of the complex and thanks to the reaction rate of the condensation of the mixed aggregate on the aldehyde, which seems by far larger than that of the pure alkyl lithium.

A parallel spectroscopic and theoretical study helped us to understand the mechanisms underlying the induction phenomena. The formation of robust 1:1 noncovalent aggregates between the 3APLi and the AlkLi derivatives could be established in THF and Et_2O . Actually, aryl- and vinyl-lithium behave similarly [14,22,23]. Multinuclear NMR and quantum mechanics both suggest that these entities are built around a $\text{N}-\text{Li}-\text{C}-\text{Li}$ quadrilateral, in which one of the two lithium cations is chelated by the nitrogen of the pyrrolidine ring. A folded norbornyle-like arrangement results from this intramolecular interaction. When the lateral chain borne by the exocyclic nitrogen is chiral, an *endo* (concave) or *exo* (convex) topology can be obtained, depending on the relative configuration of the two asymmetric centers. The sense of the asymmetric induction during the condensation of the aggregates on *o*-tolualdehyde seems to be controlled by these topologies, and thus by the configuration of the original amide.

The final steps of this reaction were then detailed by DFT calculations on model systems. This part of the work allowed us to characterize the “fully loaded” complexes resulting from the docking of the carbonyl on one of the lithium cations of the mixed aggregates. In all cases considered, early transition states are reached upon a simple rotation of the aldehyde around its $\text{C}=\text{O}$ bond, and are therefore associated to very low activation barriers ($<5 \text{ kcal mol}^{-1}$). The $\text{C}-\text{C}$ bond formation is always largely exothermic and yields a mixed aggregate of the lithium alcoholate and the remaining lithium amide. With small amides, a competitive $\text{C}-\text{N}$ bond formation occurs, and its relative rate depends on the hybridization of the nucleophile.

Hopefully, the in-depth analysis of this model reaction, conducted in parallel by experimental, spectroscopic, and theoretical means, will allow the improvement of the chiral ligands and afford a better understanding of the interactions governing the enantiodetermining step of this fundamental mode of C–C bond formation. Going further will require more sophisticated models, in particular for the interaction of the aldehyde and the “real” 3-APLi:AlkLi mixed aggregates. The important role played by the solvent will have also to be clarified. Finally, we hope that the information collected through these studies will help to design ligands [11] exhibiting new chelating patterns to be tested in other asymmetric reactions.

ACKNOWLEDGMENTS

We warmly thank Dr. Claude Giessner-Prettre (LCT, University Paris VI) for her continuous interest and strong involvement in this program. Our work on organolithium chemistry are supported by the Conseil Régional de Haute-Normandie. Computations have been performed at the CRIHAN (St-Etienne-du-Rouvray, France), IDRIS (Orsay, France), and CCR (Paris, France). A.C., N.D., and S.D. acknowledge the Ministère de la Recherche et de la Technologie for Ph.D. fellowships.

REFERENCES

1. Provided aggregation level and reactivity are unambiguously related, which is not necessary the case, as discussed in ref. 13.
2. (a) L. Pu and H. B. Yu. *Chem. Rev.* **101**, 757–824 (2001); (b) D. J. Ramon and M. Yus. *Angew. Chem., Int. Ed.* **43**, 284–287 (2004).
3. M. Asami, H. Ohno, S. Kobayashi, T. Mukaiyama. *Bull. Chem. Soc. Jpn.* **51**, 1869–1873 (1978).
4. J. P. Mazaleyrat and D. J. Cram. *J. Am. Chem. Soc.* **103**, 4585–4586 (1981).
5. S. Kanoh, H. Muramoto, K. Maeda, N. Kawaguchi, M. Motoi, H. Suda. *Bull. Chem. Soc. Jpn.* **61**, 2244–2246 (1988).
6. M. B. Eleveld and H. Hogeveen. *Tetrahedron Lett.* **25**, 5187–5190 (1984).
7. (a) G. Hilmersson and Ö. Davidsson. *J. Organomet. Chem.* **489**, 175–179 (1995); (b) G. Hilmersson and Ö. Davidsson. *J. Org. Chem.* **60**, 7660–7669 (1995); (c) P. I. Arvidsson, G. Hilmersson, Ö. Davidsson. *Chem. Eur. J.* **5**, 2348–2355 (1999); (d) P. I. Arvidsson, Ö. Davidsson, G. Hilmersson. *Tetrahedron: Asymmetry* **10**, 527–534 (1999); (e) J. E. Eriksson, P. I. Arvidsson, Ö. Davidsson. *Chem. Eur. J.* **5**, 2356–2361 (1999); (f) J. Granader, R. Sott, G. Hilmersson. *Tetrahedron: Asymmetry* **14**, 439–447 (2003).
8. (a) J. Maddaluno, A. Corruble, V. Leroux, G. Plé, P. Duhamel. *Tetrahedron: Asymmetry* **3**, 1239–1242 (1992); (b) A. Corruble, J.-Y. Valnot, J. Maddaluno, P. Duhamel. *Tetrahedron: Asymmetry* **8**, 1519–1523 (1997).
9. (a) A. Corruble, J.-Y. Valnot, J. Maddaluno, P. Duhamel. *J. Org. Chem.* **63**, 8266–8275 (1998); (b) A. Corruble, D. Davoust, S. Desjardins, C. Fressigné, C. Giessner-Prettre, A. Harrison-Marchand, H. Houte, M.-C. Lasne, J. Maddaluno, H. Oulyadi, J.-Y. Valnot. *J. Am. Chem. Soc.* **124**, 15267–15279 (2002).
10. T. Mukaiyama, K. Soai, T. Sato, H. Shimizu, K. Suzuki. *J. Am. Chem. Soc.* **101**, 1455–1460 (1979).
11. N. Dugué, J. Chen, S. Petit, P. Marchand, A. Harrison-Marchand, J. Maddaluno. To be published.
12. A. Corruble, J.-Y. Valnot, J. Maddaluno, Y. Prigent, D. Davoust, P. Duhamel. *J. Am. Chem. Soc.* **119**, 10042–10048 (1997).
13. D. L. Collum. *Acc. Chem. Res.* **25**, 448–454 (1992).
14. Y. Yuan, S. Desjardins, A. Harrison-Marchand, H. Oulyadi, C. Fressigné, C. Giessner-Prettre, J. Maddaluno. *Tetrahedron* **61**, 3325–3334 (2005).

15. (a) W. Bauer. In *Lithium Chemistry: A Theoretical and Experimental Overview*, A. M. Sapse and P. v. R. Schleyer (Eds.), p. 125, John Wiley, Chichester (1995); (b) H. Günther. *J. Braz. Chem. Soc.* **10**, 241–262 (1999).
16. O. Parisel, C. Fressigné, J. Maddaluno, C. Giessner-Prettre. *J. Org. Chem.* **68**, 1290–1294 (2003).
17. (a) J. F. Mc Garrity and C. A. Ogle. *J. Am. Chem. Soc.* **107**, 1805–1810 (1985); (b) J. F. Mc Garrity, C. A. Ogle, Z. Brich, H.-R. Loosli. *J. Am. Chem. Soc.* **107**, 1810–1815 (1985).
18. See *inter alia*: (a) L. M. Pratt and I. M. Khan. *J. Comp. Chem.* **16**, 1067–1080 (1995); (b) O. Kwon, F. Sevin, M. L. McKee. *J. Phys. Chem. A* **105**, 913–922 (2001); (c) L. Pratt, N. V. Nguyễn, B. Ramachandran. *J. Org. Chem.* **70**, 4279–4283 (2005).
19. (a) C. Fressigné, J. Maddaluno, A. Marquez, C. Giessner-Prettre. *J. Org. Chem.* **65**, 8899–8907 (2000); (b) C. Fressigné, A. Lautrette, J. Maddaluno. *J. Org. Chem.* **70**, 7816–7828 (2005).
20. (a) P. Zhao, A. Condo, I. Keresztes, D. B. Collum. *J. Am. Chem. Soc.* **126**, 3113–3118 (2004); (b) For applications of α -aminoalcoholates in synthesis, see D. L. Comins. *Synlett* 615–625 (1992).
21. A. E. Dorigo and K. Morokuma. *J. Am. Chem. Soc.* **111**, 4635–4643 (1989).
22. Y. Yuan, A. Harrison-Marchand, J. Maddaluno. *Synlett* 1515–1518 (2005).
23. A. Lautrette, Y. Yuan, H. Oulyadi, A. Harrison-Marchand, J. Maddaluno. To be published.